FINAL REPORT

Grant NAG 3-1032
NASA - Lewis Research Center

"TURBULENCE MODELING IN SHOCK WAVE/TURBULENT BOUNDARY LAYER INTERACTIONS"

By

A. J. Smits
Gas Dynamics Laboratory
Department of Mechanical and Aerospace Engineering
Princeton University
Princeton, N. J. 08544

Covering the Period 4/5/89 through 4/4/92

Attn: Dr. Chi R. Wang
21000 Brookparke Rd, Cleveland OH 44135

October 1992

"Turbulence Modeling in Shock Wave/Turbulent Boundary Layer Interactions"

by

A. J. Smits
Gasdynamics Laboratory
Department of Mechanical & Aerospace Engineering
Princeton University
Princeton, N.J. 08544

Summary

This is the final technical report for NASA Grant 3-1032. The research performed under this grant was an experimental program to help develop turbulence models for shock wave boundary layer interactions. The measurements were taken in a Mach 3, 16^{o} compression corner interaction, at a unit Reynolds number of 63 x 10^{6}/m. The data consisted of heat transfer data taken upstream and downstream of the interaction, hot wire measurements of the instantaneous temperature and velocity fluctuations to verify the Strong Reynolds Analogy, and single- and double-pulsed Rayleigh scattering images to study the development of the instantaneous shock/turbulence interaction.

1. INTRODUCTION

The aim of this research work was to perform experimental work which will benefit the NASA-Lewis effort to improve turbulence models for complex supersonic flows. In particular, we were interested in developing the capacity to make accurate calculations of shock wave turbulent boundary layer interactions.

NASA-Lewis Grant NAG 3-1032 "Turbulence Modeling in Shock Wave Turbulent Boundary Layer Interactions" started on 4/5/89, with the aim of improving the prediction of the flow-field features of unseparated interactions. Attention has focussed primarily on the investigation of a Mach 3, 16 degree compression corner interaction, at a unit Reynolds number of 63 x 10^6/m. Since the research was directed towards a fundamental understanding of the flow field behavior, and the development of scaling laws for changes in Mach number and Reynolds number, we expect that the results will be applicable over a wide range of conditions, especially at higher Mach number.

The particular shock-wave boundary layer interaction selected for study under this Grant has been investigated in the past by Settles, Fitzpatrick and Bogdonoff (1979), who documented the mean flow, and Smits and Muck (1987), who studied aspects of the turbulence evolution. Nevertheless, our understanding of this flow, and other complex flows, is still rather limited. As a result, the computations display severe shortcomings. These inadequacies were well documented at the Stanford Conference on Complex Turbulent Flows (Kline et al. 1981), and in broad terms the situation has not improved very much in the intervening decade. The situation is well illustrated by the results reported for compression corners by Visbal and Knight (1983) and for curved wall compressions by Degani and Smits (1990). See Figure 1 for some typical results. Algebraic turbulence model are usually inadequate, but it is not immediately clear how better results may be obtained. One- or two-equation models can lead to better results, but only under some circumstances (Horstman et al. 1977, Degani and Smits 1990), and currently it appears that no fully reliable methods are available for the prediction of these complex flows.

One of assumptions commonly made in developing turbulence models for high speed flows deserves some particular attention, that is, the assumption that the temperature and velocity fields are coupled according to the Strong

Reynolds Analogy (SRA), which states that:

The analysis by Smits et al. (1989) suggested that there must exist some phase difference between the density and velocity fields, even in an undisturbed boundary layer. In the present study, the instantaneous form of the SRA was tested for the first time in any flow. It was studied both in the undisturbed Mach 2.9 high-Reynolds-number turbulent boundary layer upstream of the 16^{o} compression corner, and in the strongly perturbed flow downstream of the shock-wave/boundary layer interaction (Smith and Smits, 1990, 1992).

Another aspect to consider in modelling these flows is the unsteadiness of the shock. Shock-wave unsteadiness appears to be a characteristic feature of shock wave boundary layer interactions, in two and three dimensions (see, for example, Dolling and Dussauge 1990), and it may exert a considerable distorting influence on the turbulence behavior in the downstream flow (Smits and Muck 1987). In the present study, the interaction of the turbulence with the shock was studied using Rayleigh scattering, which makes possible the imaging of the instantaneous density field. The spanwise wrinkling of the shock (previously inferred from spanwise wall pressure measurements by Muck, Dussauge and Bogdonoff 1985) was visualized using this technique (Smith et al. 1990). These observations were the first of their kind in this class of interactions. These data have been extended recently to visualize the compression and distortion of turbulent motions as they pass through the shock (Forkey et al. 1993).

Finally, the wall heat transfer in shock wave boundary layer interactions is not often studied, and the calculation of heat transfer rates usually requires the assumption of some form of the Reynolds Analogy. The measurements of the mean heat transfer were reported by Evans and Smits (1992) and Evans (1992). The results indicate that the Reynolds Analogy factor increases by over 70% through the interaction and shows no sign of relaxation.

2.2 Experimental Conditions

The experiments were conducted in the 8" x 8" Mach 3 blowdown tunnel at the Gasdynamics Laboratory of Princeton University. Tests were made on the tunnel floor at where the incoming boundary layer was approximately 1.0"

thick. The boundary layer was fully turbulent. Transition occurred naturally, and no trips were used. A 16^{o} compression ramp was used to generate the interaction. Data were taken at one flow condition, namely a stagnation pressure of 100 psia, generating a nominal freestream Reynolds number of 63 million per meter (19 million per foot). See also Table 1.

2.3 Results

The simultaneous measurements of the temperature and velocity fluctuations were obtained using a new dual sensor hot wire probe (Smith and Smits 1990). Here, both hot wires are operated in the constant temperature mode, one at an overheat ratio of 1.1, and the other at an overheat ratio of 0.3 or 0.4. Under these operating conditions the signals may be decomposed into velocity and density. The time-averaged results are in good agreement with previous data at similar Mach numbers, giving some confidence in the accuracy of the technique. The time-averaged data are given in figures 2 and 3. Some time traces of velocity and temperature are shown in figure 4, and the strong correlation between the two signals is obvious. The correlation coefficients shown in figure 5 are close to one, and the validity of the instantaneous (and time-averaged) form of the SRA seems confirmed for this flow, even in the highly disturbed flow field downstream of the interaction.

Instantaneous, quantitative visualization of the density field in a cross-section of the flow using Rayleigh scattering (Smith et al. 1990). An example of an image obtained using this technique is shown in figure 6. This image was made possible by using a high-power, Nd:YAG laser operating in the far-ultraviolet in conjunction with a high-sensitivity, far-ultraviolet camera. By focusing the laser into a thin sheet of light and passing it through the wind tunnel, cross-sectional images of the air density can be recorded by direct Rayleigh scattering. For the pictures shown here, the illumination is with a Quantel International YG661 laser operating in the vicinity of .266 microns with a pulse duration of 4 nsec, so the cross-sectional image is frozen in time. The 8"x8" Mach 2.9 tunnel was fitted with UV transmitting quartz windows so that the laser sheet could be passed through the flow field. The high-sensitivity camera observed the scattering at 90^{o} and images could be recorded up to the camera framing rate of 10 Hz.

The presence of water can have a strong effect on the interpretation of

these images, even for extremely low water concentrations (parts per million). Upstream of the nozzle, where the water is in the form of water vapor, its Rayleigh cross section is small. As the flow expands through the nozzle, the water molecules can agglomerate into very small ice crystals of the order of 30 nanometers in diameter (Wegener and Stein 1968), and these small particles dominate the Rayleigh signal. Quantitatively, therefore, the images show the density of these ice crystals rather than the density of air. Now, it appears that the ice crystal density is nearly proportional to the local air density, except in regions where the temperature rises to the point where the ice returns to the vapor phase. There are two main consequences: we lose some resolution near the wall, where the frictional heating increases the temperature, and strong shocks become visible as lines separating bright zones (low temperature) from dark zones (high temperature).

For each image shown in figure 6a, the Reynolds number, based on the incoming boundary layer momentum thickness, was about 80,000. The scale, from top to bottom, is about 60 mm and the resolution is on the order of several hundred microns. The boundary layer thickness is approximately 28 mm. The flow is from right to left, and the images show the incoming boundary layer on the left, the unsteady separation shock (the line coming down from the left), and the highly distorted compressed boundary layer downstream of the shock.

In a qualitative fashion, these images show that there are well-defined individual structures located in the incoming boundary layer. The dark areas of the image represent low density regions characteristic of high temperatures. The bright areas are the high densities found in the free stream. Intermittent penetration of freestream fluid deep into the boundary layer is clearly visible. These large scale motions can interact strongly with the shock wave, as shown in the figures, and it appears that the unsteady shock motion is closely coupled with the strength and frequency content of the incoming boundary layer structure. Spanwise images (an example, taken in a 24o corner flow, is given in figure 6b) clearly show the spanwise rippling of the shock sheet. As far as we know, these images are the first to reveal the instantaneous shock structure in compression corner interactions, and the first to show the strong influence of the turbulence on the unsteady shock motion. At this stage, the particular characteristics of the turbulence that result in the strong coupling is

not known, although we suspect that only large motions, with a high degree of coherence can interact directly with the shock. Further data analysis may lead to deeper insights. For example, image processing techniques can be used to generate space correlations of the fluctuating density field, and reveal the dynamic connection between the incoming motions, the shock motion, and the turbulence distortion.

More recent work has used double-pulsed Rayleigh imaging to visualize the evolution of the turbulent boundary layer motions (Cogne et al. 1993), and the distortion of the incoming motions as they pass through the shock generated by the 16^{o} compression corner. The strong shearing and compression experienced by the incoming turbulence is evident from the images (see Figure 7 for a typical image).

Thin film heat transfer gauges were used to measure the mean wall heat transfer rates in the boundary layer. These data were obtained using an array of eight gauges are being used, supplied by Dr. Mike Dunn of Calspan. These are platinum sensors, with a thickness of 0.15 micron and a spatial resolution of approximately 1 mm. They were operated in a constant current mode, with a current of 3 mA, and the frequency response was calculated to be in excess of 1 MHz, although noise considerations reduce the useful bandwidth to something less than 200 Hz-200 kHz. The primary question was whether these gauges are sensitive enough, and have sufficient frequency response, to allow accurate heat transfer measurements in this flow, without heating or cooling the wall, that is, in near-adiabatic conditions (the difference between the ambient temperature and the recovery temperature is of the order of a few degrees). Data were obtained in the upstream boundary layer, and downstream on the ramp face (Evans and Smits 1992, Evans 1992). A correction scheme was devised to account for the fall in stagnation temperature during the run, and for the breakdown of the semi-infinite assumption in the data reduction (Evans 1992). The results, shown in Figures 8-10, seem to indicate that accurate Stanton number values can be obtained. The most impressive result is the large increase in the Reynolds Analogy factor observed through the interaction. At the present time, the signal-to-noise ratio is too high to enable accurate measurements of the instantaneous heat transfer rate to be made.

2.4 Conclusions

For the Mach 3, 16^{o} compression corner flowfield studied here:

1. The Strong Reynolds Analogy applies to a high level of accuracy, even in the instantaneous sense.
2. Strong turbulence/shock interactions have been observed using Rayleigh scattering, including the spanwise rippling of the shock sheet.
3. It is possible to obtain accurate mean heat transfer data using thin-film gauges in this flow, without heating or cooling the wall.
4. The compression and shearing of turbulence by the interaction with a shock has been observed directly using double-pulsed Rayleigh scattering.

2.5 Publications Acknowledging This Grant

Smith, D.R., Poggie, J. and Smits, A.J., "Application of Rayleigh Scattering to Supersonic Turbulent Flows", Proc. Fifth International Symposium on Applications of Laser Techniques to Fluid Mechanics, July 9-12 1990, Lisbon, Portugal. To be published Springer Verlag, 1991.

Smits, A.J., "An Introduction to Hot-Wire Anemometry in Flows", Proc. Symp. on the Heuristics of Thermal Anemometry, ASME Fluids Engineering Div. Spring Meeting, Toronto, Ontario, Canada, 1990. ASME Publication FED-Vol. 97, Ed. D.E. Stock, S.A. Sherif and A.J. Smits.

Smith, D.R., Poggie, J., Konrad, W. and Smits, A.J., "Visualization of the Structure of Shock Wave Turbulent Boundary Layer Interactions Using Rayleigh Scattering", AIAA Paper #91-0651, AIAA 29th Aerospace Sciences Meeting, Reno, Nevada, January 1991.

Smith, D.R. and Smits, A.J., "Velocity and Temperature Measurements in a Mach 3 Turbulent Boundary Layer," Paper #IA6, 43rd Annual Meeting, Division of Fluid Dynamics, American Physical Society, November 1990. Submitted to Journal of Experimental Thermal and Fluid Science, 1992.

Evans, T. and Smits, A.J., "Measurements of the Mean Heat Transfer in a Shock Wave Turbulent Boundary Layer Interaction," Proceedings Thirteenth Symposium on Turbulence, University of Missouri-Rolla, September 21-23, 1992.

T. Evans, "Heat Transfer in a Two-Dimensional Shock Wave Turbulent Boundary Layer Interaction" MSE Thesis, Department of Mechanical and Aerospace Engineering, Princeton University, 1992.

Forkey, J., Cogne, S., Smits, A.J., Bogdonoff, S.M., Lempert, W. and Miles, R.B. "Visualization of Shock-Turbulence Interactions in Two- and Three-Dimensional Flows Using Double-Pulsed Rayleigh Scattering". To be presented AIAA Propulsion Meeting, Monterey, CA, July 1993.

REFERENCES and BIBLIOGRAPHY

Alving, A. E. 1988 "Boundary layer relaxation from convex curvature," Ph.D. Thesis, Princeton Univ., Princeton, NJ.

Blackwelder, R. and Kaplan, R. E. 1976 "On the wall structure of the turbulent boundary layer," J. Fluid Mech. 76,89.

Brown, G. L. and Thomas, A. S. W., [1977], Large structure in a turbulent boundary layer, Physics of Fluids, Vol. 20(10), p. 243.

Deckker, B. E. L. [1980], Boundary layer on a shock tube wall and at a leading edge using schlieren, Second International Symposium on Flow Visualization, Ruhr-Universitat Bochum, West Germany. Ed. W. Merzkirch, Hemisphere, p. 413.

Deckker, B. E. L. and Weekes, M. E. [1976], The unsteady boundary layer in a shock tube, Proc. I. Mech. Eng., Vol. 190, p. 287.

Dolling, D. S. and Murphy, M. T. (1983), "Unsteadiness of the Separation Shock Wave in a Supersonic Compression Ramp Flowfield," AIAA Journal, Vol. 21, pp. 1628-1634.

Donovan, J. F. and Smits, A. J. [1987], A preliminary investigation of large-scale organized motions in a supersonic turbulent boundary layer on a curved surface, AIAA Paper 87-1285.

Dolling, D.S. and Dussauge, J.P., "Fluctuating Wall-Pressure Measurements", Chapter 8, NATO AGARDograph #315, 1989

Dussauge, J.P., Debieve, J.F. and Smits, A.J., "Rapidly Distorted Compressible Boundary Layers", Chapter 2, NATO AGARDograph #315, 1989

Dussauge, J. P. and Gaviglio, J. [1981], Bulk dilatation effects on Reynolds stress in the rapid expansion of a turbulent boundary layer at supersonic speed, Proc.Third Symposium on Turbulent Shear Flows, Univ. Cal., Davis.

Dussauge, J. P. and Gaviglio, J. 1987 "The rapid expansion of a supersonic turbulent flow: role of bulk dilatation, "J. Fluid Mech. 174, p. 81.

Fernando, E. M. 1988 "The effects of an adverse pressure gradient on a flat plate, supersonic, turbulent boundary layer," Ph.D. Thesis, Princeton Univ., Princeton, NJ.

Fernando, E. M. and Smits, A. J. [1987], The effects of an adverse pressure gradient on the behavior of a supersonic turbulent boundary layer, AIAA Paper 87-1286.

Fernando, E. M., Spina, E. F., Donovan, J. F. and Smits, A. J. [1987], Detection of large-scale organized motions in a turbulent boundary layer, Sixth Symposium on Turbulent Shear Flows, Toulouse, France.

Fernholz, H. H. and Finley, P. J. 1980 "A critical commentary of compressible turbulent boundary layer data," AGARDograph No. 253.

Fernholz, H.H., Smits, A.J., Dussauge, J.-P. and P.J. Finley, (Eds.), "A Survey of Measurements

and Measuring Techniques in Rapidly Distorted Compressible Turbulent Boundary Layers," NATO-Advisory Group for Aerospace Research and Development AGARDograph, #315, 1989.

Fernholz, H.H. and Smits, A.J., "Introduction", Chapter 1, NATO AGARDograph, #315, 1989

Head, M. R. and Bandyopadhyay, P. [1981], New aspects of turbulent boundary-layer structure, Journal of Fluid Mechanics, Vol. 107, p. 297.

Hayakawa, K., Smits, A. J. and Bogdonoff, S. M. (1984), "Hot-Wire Investigation of an Unseparated Shock-Wave/Turbulent Boundary-Layer Interaction," AIAA Journal 22, pg. 579.

Horstman, C. C., Settles, G. S., Vas, I. E., Bogdonoff, S. M. and Hung, S. M. (1977), "Reynolds Number Effects on Shock Wave Turbulent Boundary Layer Interactions," AIAA Journal, Vol. 15, pp. 1152-1158.

James, C. S. (1958), Observations of turbulent-burst geometry and growth in supersonic flow, NASA TN 4235.

Johansson, A. V. and Alfredson, p. H. [1982], On the structure of turbulent channel flow, Journal of Fluid Mechanics, Vol. 122, p. 295.

Karniadakis, G. E., Mikic, B. B. and Patera, A. T. (1988), "Minimum Dissipation Transport Enhancement by Flow Destabilization: Reynolds' Analogy Revisited," J. Fluid Mech., 192:365.

Kistler, A. L. 1959 "Fluctuation measurements in a supersonic turbulent boundary layer," Phys. Fluids 2, 290.

Kovasznay, L. S. G., Kibens, V. and Blackwelder, R. F. 1970 "Large-scale motion in the intermittent region of a turbulent boundary layer," J. Fluid Mech. 41, 283.

Lu, L. J. and Smith, C. R. (1985), "Image Processing of Hydrogen Bubble Flow Visualization for Determination of Turbulence Statistics and Bursting Characteristics," Expts. in Fluids, 3:349.

Miles, R., Connors, J., Howard, P., Markovitz, E. and Roth, G. (1988a), "Proposed Single-Pulse, Two-Dimensional Temperature and Density Measurements of Oxygen and Air," Optics Letters 13, pg. 195.

Miles, R., Connors, J., Markovitz, E., Howard, P. and Roth, G. (1988b), "Instantaneous Supersonic Velocity Profiles in an Underexpanded Jet by Oxygen Flow Tagging," (Accepted for publication in Physics of Fluids).

Moin, P. and Kim, J. [1985], The structure of the vorticity field in turbulent channel flow. Part 1 - analysis of instantaneous fields and statistical correlations, Journal of Fluid Mechanics, Vol. 155, p. 441.

Morkovin, M. V. 1962 "Effects of compressibility on turbulent flows," Int. Symp. on the Mechanics of Turbulence 367. C.N.R.S., Paris.

Nosenchuck, D. M. and Lynch, M. K. (1986), "Three-dimensional Flow Visualizations Using Laser-Sheet Scanning," In Proc. AGARD Conf. on Aerodynamics and Related Hydrodynamics Studies Using Water Facilities, pg. 18.1.

Owen, F. K. and Horstman, C. C. [1981], Turbulent measurements in an equilibrium hypersonic boundary layer, AIAA Paper 74-93.

Owen, F. K., Horstman, C.C. and Kussoy, M. I. 1975 "Mean and fluctuating flow measurements of a fully developed, non-adiabatic hypersonic boundary layer," J. Fluid Mech. 70, 393.

Perry, A. E. and Chong, M. S. [1982], On the mechanism of wall turbulence. Journal of Fluid Mechanics, Vol. 119, pp. 173-217.

Rajagopalan, S. and Antonia, R. A. [1979], Some properties of the large structure in a fully developed turbulent duct flow, Physics of Fluids, Vol. 22(4), p. 614.

Robinson, S. K. [1985], Instantaneous velocity profile measurements in a turbulent boundary layer, Chem.Eng. Communications, Vol. 43, p. 347.

Robinson, S. K. [1986], Space-time correlation measurements in a compressible turbulent boundary layer, AIAA Paper 86-1130.

Russell, G. and Miles, R. B. (1987), "Display and Perception of Three-Dimensional Space Filling Data", Applied Optics 26: 973.

Sabadell, L. A., Watmuff, J. H. and Smits, A. J. (1989), "Modification of Turbulence Structure by a Drag-Reducing Surfactant Solution," in Second IUTAM Symp. on Structure of Turbulence and Drag Reduction, ETH, Zurich.

Selig, M. S., Andreopoulos, J., Muck, K. C., Dussauge, J. P. and Smits, A. J. (1989), "Turbulence Structure in a Shock Wave/Turbulent Boundary Layer Interaction," to be published in AIAA Journal, January.

Settles, G. S., Vas, I. E. and Bogdonoff, S. M. (1976), Details of a Shock-Separated Turbulent Boundary Layer at a Compression Corner," AIAA Journal, Vol. 14, pp. 1709-1715.

Smits, A. J. and Muck, K. C. [1986], Experimental study of three shock wave/turbulent boundary layer interactions. Journal of Fluid Mechanics, Vol. 182.

Smits, A.J. and Watmuff, J.H., "Large-Scale Motions in Supersonic Turbulent Boundary Layers", Chapter 3, NATO AGARDograph, #315, 1989

Smits, A.J. and Dussauge, J.P.,"Hot-Wire Anemometry in Supersonic Flows", Chapter 5, NATO AGARDograph, #315, 1989

Smith, C. R. [1984], A synthesized model of near-wall behavior in turbulent boundary layers, Proceedings of Eighth Symposium on Turbulence, (Ed. G. K. Patterson and J. L. Zakin), Department of Chemical Engineering, University of Missouri-Rolla).

Smith, M. W., Kumar, V., Smits, A. J. and Miles, R. B. (1989), "The Structure of Supersonic Turbulent Boundary Layers as Revealed by Line Profiles and Density Cross Sections," to be presented, Seventh Symposium on Turbulent Shear Flows, Stanford University, Stanford, CA.

Smith, M. W. and Smits, A. J. 1988 "Cinematic visualization of coherent density structures in a supersonic turbulent boundary layer," AIAA Paper 88-500.

Smits, A. J., Alving, A. E., Smith, R. W., Spina, E. F., Fernando, E. M. and Donovan, J. F. (1988), "A Comparison of the Turbulence Structure of Subsonic and Supersonic Boundary Layers," Proc. Eleventh Symp. on Turbulence, Univ. Missouri-Rolla, Rolla, Missouri.

Smits, A. J., Hayakawa, K. and Muck, K. C. [1983], "Constant-temperature hot-wire anemometer practice in supersonic flows. Part I - The normal wire, Experiments in Fluids, Springer-Verlag.

Smits, A. J., Muck, K. C. and Hayakawa, K. 1983 "Constant temperature hot-wire anemometry practice in supersonic flows, Part I: The normal wire," Experiments in Fluids 1, 83.

Spalart, P. R. (1988), "Direct Simulation of a Turbulent Boundary Layer up to Re = 1410," J. Fluid Mech. 187: 61.

Spina, E. F. 1988 "Organized Structures in a Supersonic Turbulent Boundary Layer" Ph. D. Thesis, Princeton Univ., Princeton, NJ.

Spina, E. F. and Smits, A. J., [1986] "Organized structures in a supersonic turbulent boundary layer", Princeton University, Dept. of Mechanical and Aerospace Engineering, Report #1736.

Spina, E. F. and Smits, A. J. (1987), "Organized Structures in a Compressible Turbulent Boundary Layer," Journal of Fluid Mechanics, 182:85-109.

Thomas, A. S. W. and Bull, M. K. [1983], On the role of wall-pressure fluctuations in deterministic motions in the turbulent boundary layer, Journal of Fluid Mechanics, Vol. 128, p. 283.

Tran, T. T. 1987 "An experimental investigation of unsteadiness in swept shock wave/turbulent boundary layer interactions," Ph.D. Thesis, Princeton Univ., Princeton, NJ.

van Driest, E. R. 1951 "Turbulent boundary layer in compressible fluids," Journal of
Van Dyke, M. [1982], An Album of Fluid Motion, The Parabolic Press, Stanford, CA. Aeronautical Sciences 128, 283.

Wegener P. P. and Stein, G. D. 1968 "Light-Scattering Experiments and Theory of Homogeneous Nucleation in Condensing Supersonic Flow," 12th International Symposium on Combustion, 1183-119.

p_o (Nt/m^2)	6.8×10^5
T_o (^{o}K)	265 ± 5
M_e	2.84 ± 0.04
U_e (m/s)	575 ± 20
$(\rho U)_e$ (kg/m^{2}s)	500 ± 30
Re_e/m	$6.5 \pm 0.5 \times 10^7$
(mm)	26 ± 1.5
C_f	$.001 \pm .0001$

Table 1. Flat plate, zero pressure gradient, adiabatic wall, turbulent boundary layer (Spina & Smits 1987).

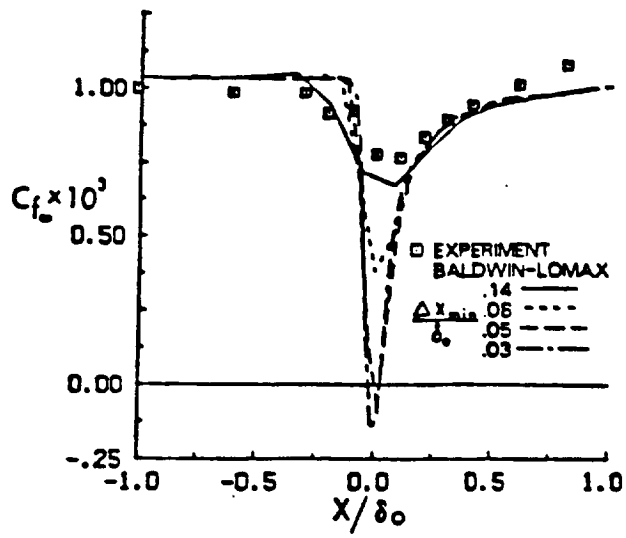

Skin friction coefficient for 8° ramp (Re_{δ_o} = 1.6 x 10^6).

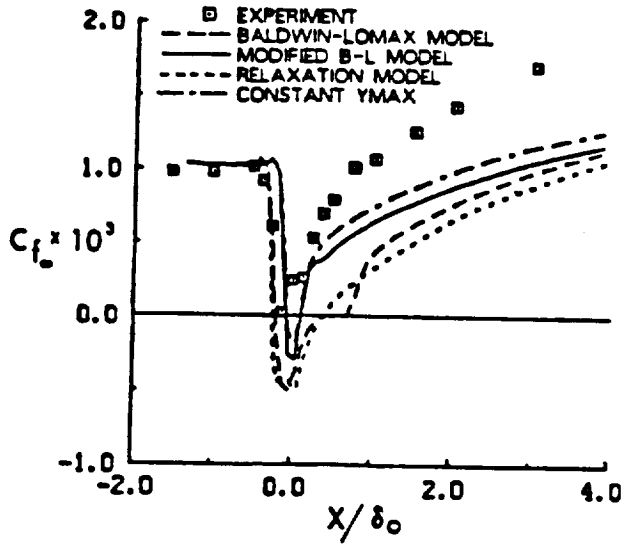

Skin friction coefficient for 16° ramp (Re_{δ_o} = 1.6 x 10^6).

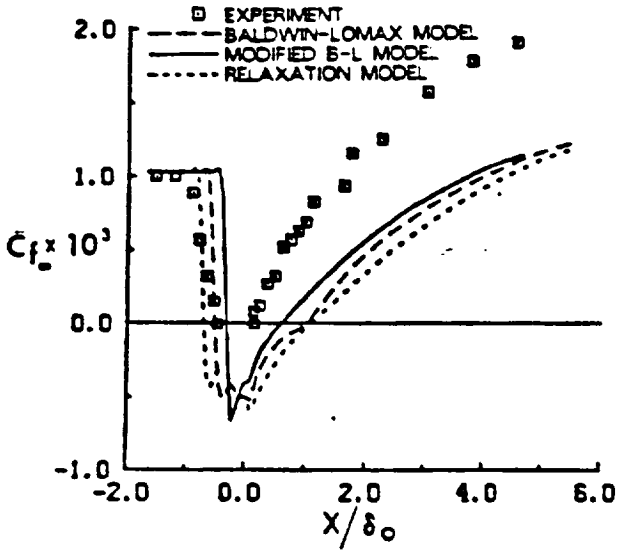

Skin friction coefficient for 20° ramp (Re_{δ_o} = 1.6 x 10^6).

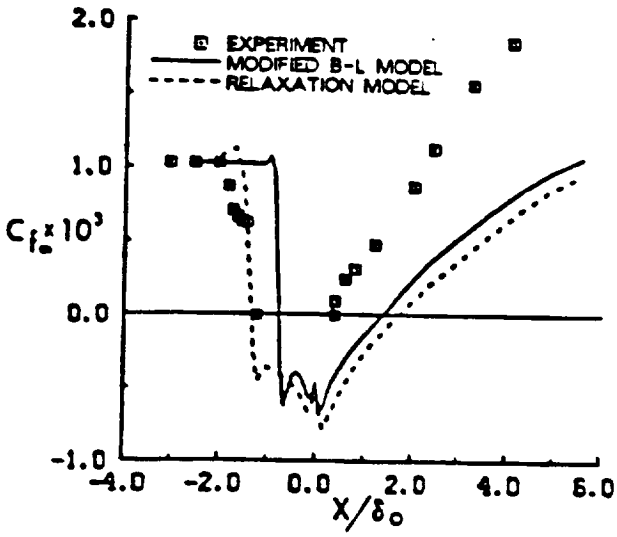

Skin friction coefficient for 24° ramp (Re_{δ_o} = 1.6 x 10^6).

Figure 1. Comparison between experiment (Settles et al. 1978) and computation (Visbal and Knight 1983) for Mach 2.9 compression corner flows.

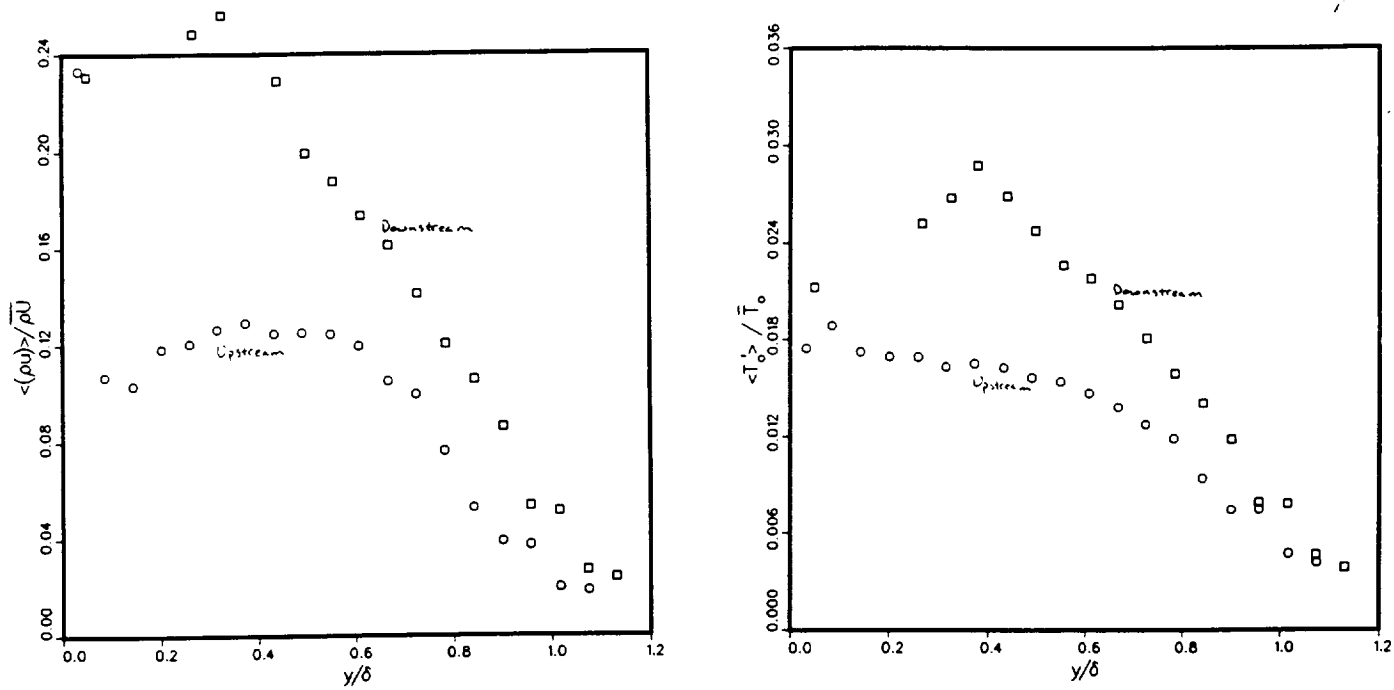

Figure 2. Results from dual hot-wire technique. Mass-flux and temperature rms levels. Circles represent incoming boundary layer data, squares represent data taken 2.8delta downstream of the corner. Incoming boundary layer parameters given in Table 1.

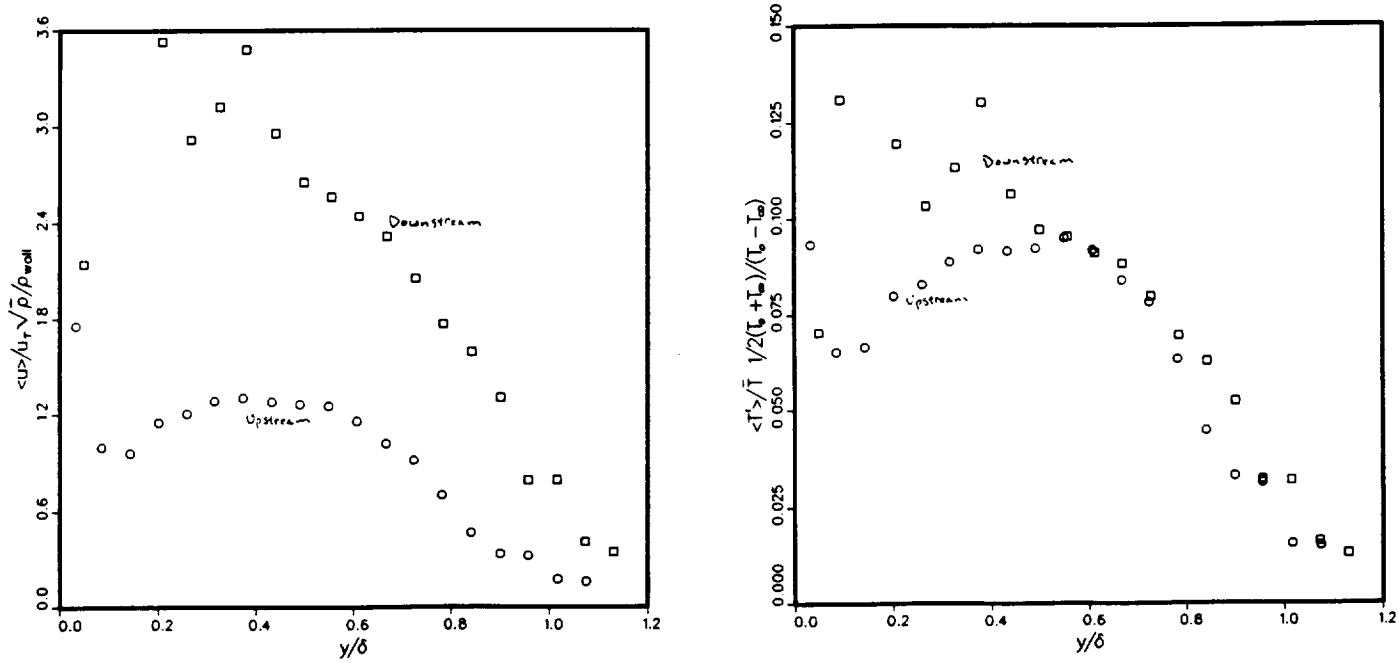

Figure 3. Results from dual hot-wire technique. Velocity and temperature rms levels in similarity coordinates. Circles represent incoming boundary layer data, squares represent data taken 2.8delta downstream of the corner. Incoming boundary layer parameters given in Table 1.

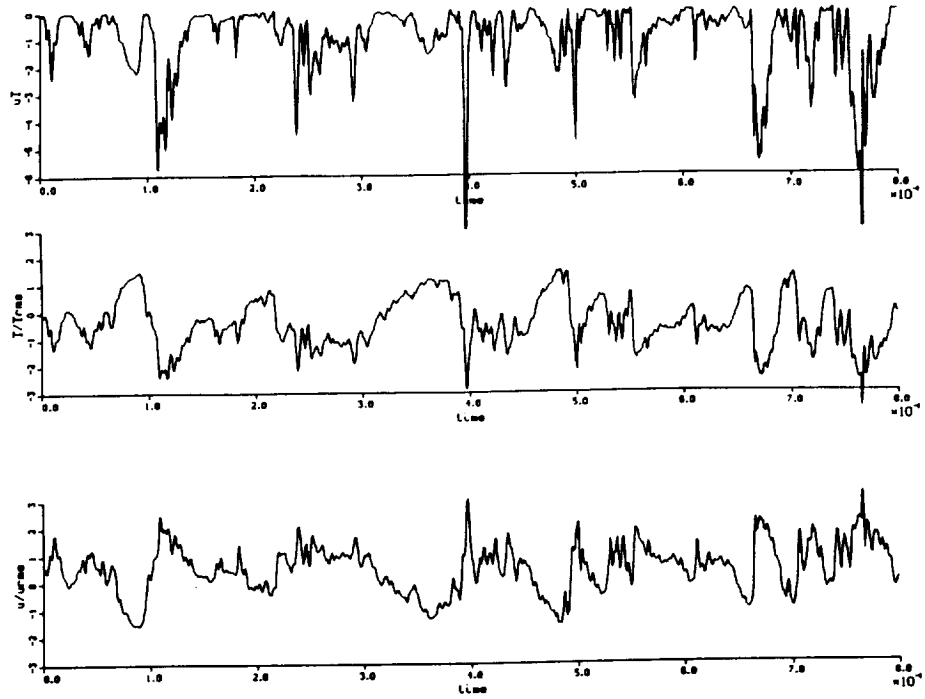

Figure 4. Results from dual hot-wire technique. Time traces of velocity, temperature and the velocity-temperature product, taken 2.8delta downstream of the corner at y/delta = 0.7.

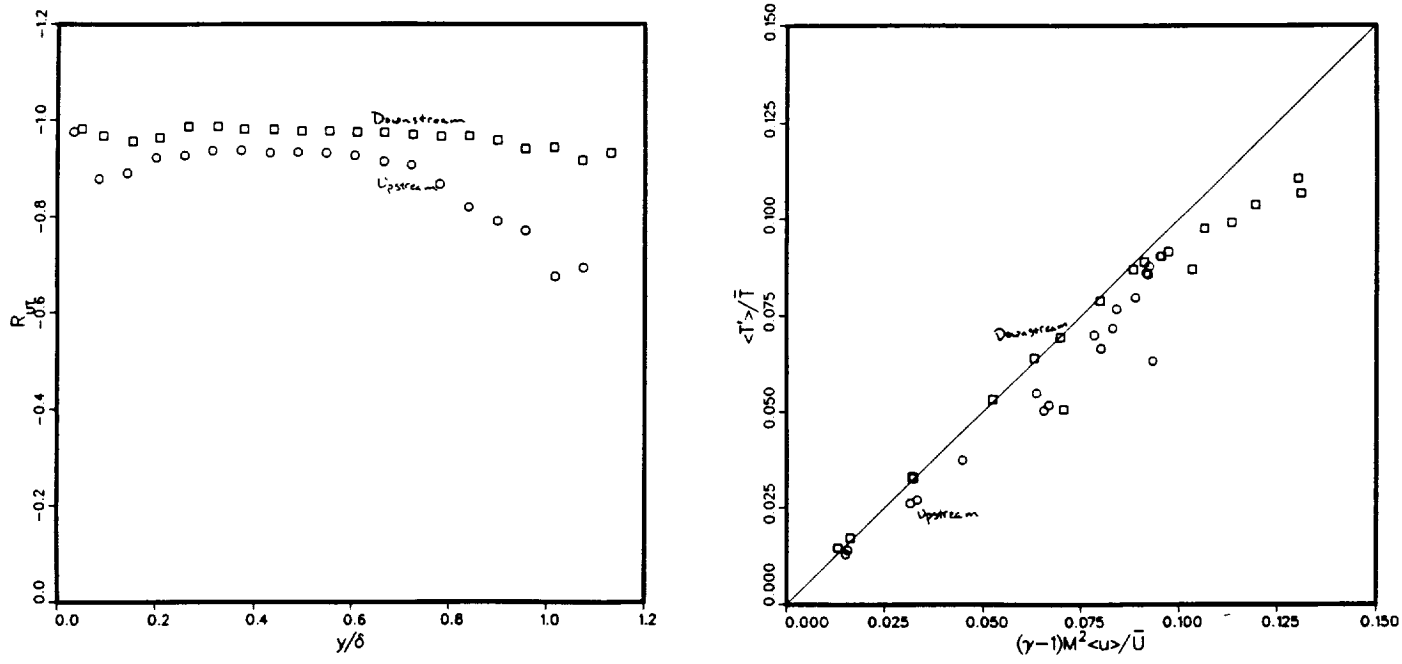

Figure 5. Results from dual hot-wire technique. (a) correlation coefficient R_{uT}; (b) time-averaged form of the SRA. Circles represent incoming boundary layer data, squares represent data taken 2.8delta downstream of the corner.

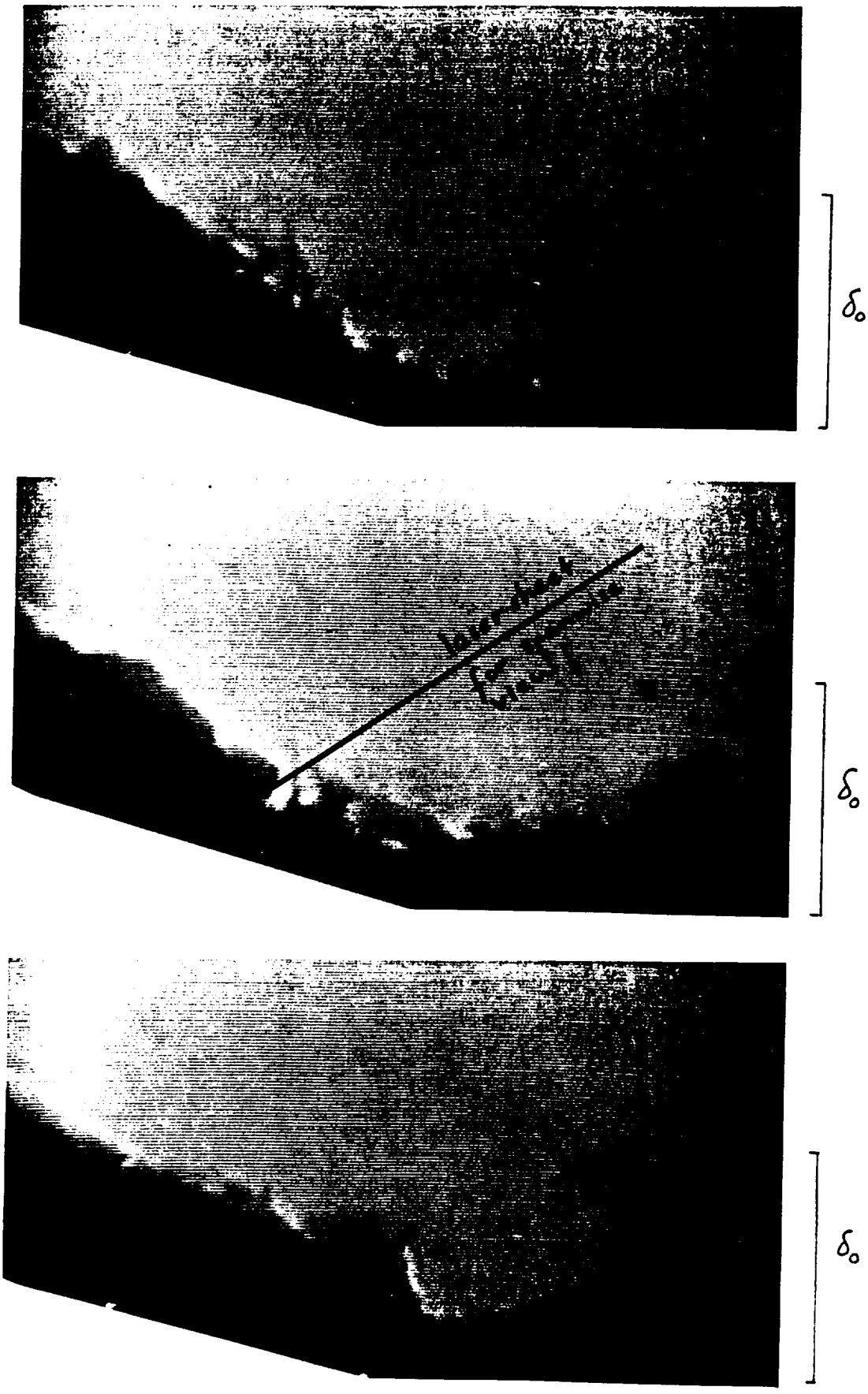

Figure 6a. Images of shock wave boundary layer interaction obtained using Rayleigh scattering technique. Flow over the 16^o ramp is from right to left. The intensity is a measure of the local density. Incoming boundary layer conditions are as given in Table 1.

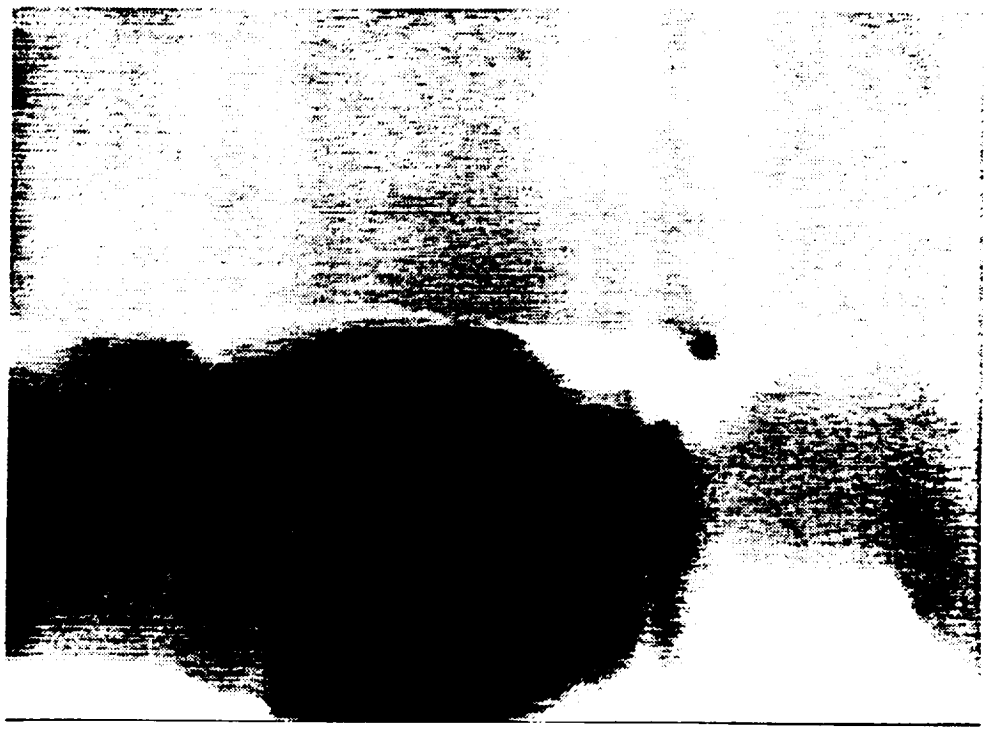

Figure 6b. Spanwise Rayleigh image in a 24^{o} ramp air flow, downstream of the corner. The laser sheet orientation is shown in Figure 6a. Flow is from top to bottom of the picture. Shocks show up as regions where the brightness increases (this is true as long as the temperature rise is relatively small). These images indicate that more than one shock is present in the attachment region, and that they are strongly wrinkled by the incoming turbulence.

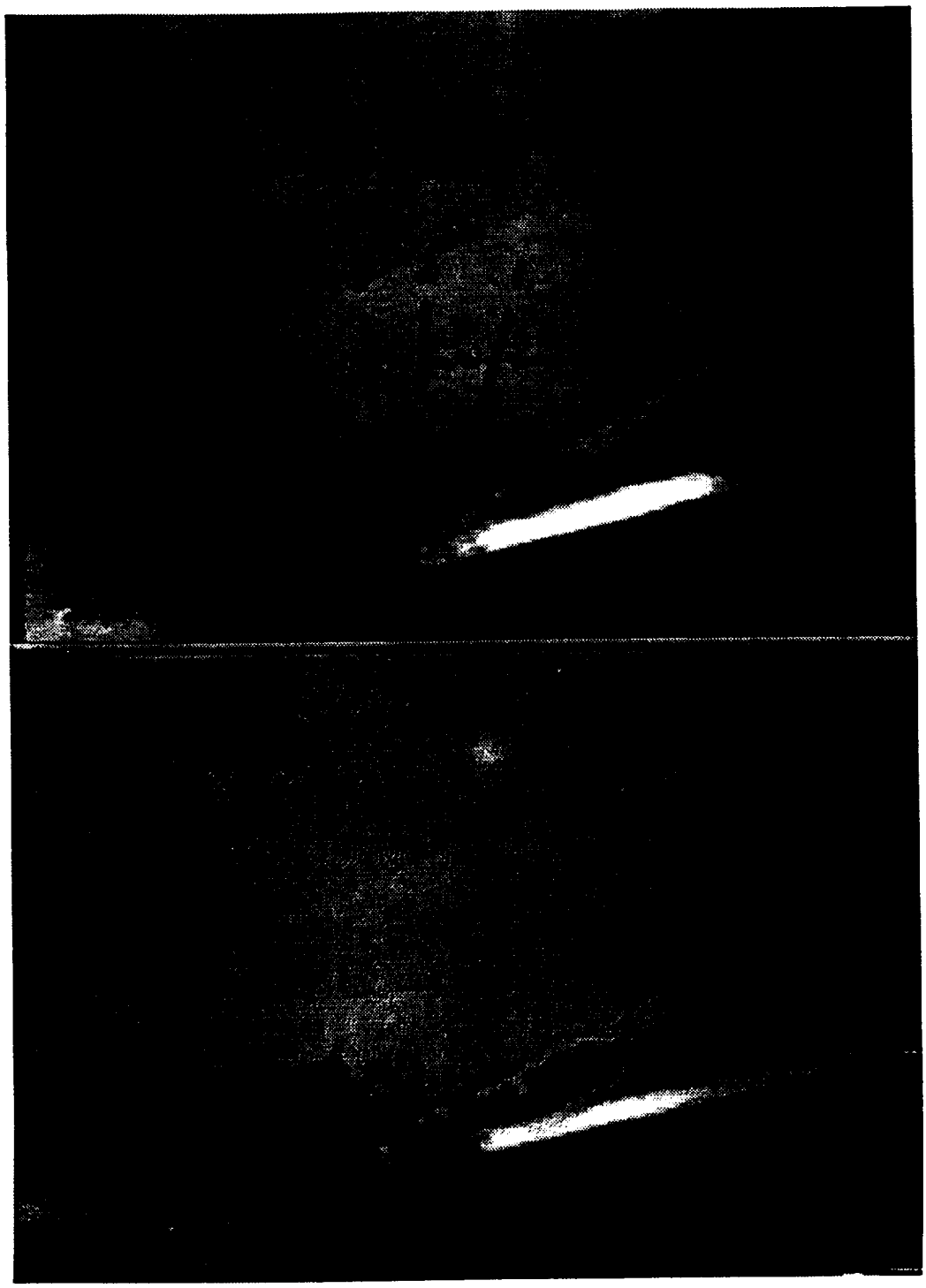

Figure 7. Two Rayleigh scattering images obtained in the 16^{o} compression corner flow, where the bottom image is separated in time from the top image by 40 microseconds. Flow is from left to right. The numbers refer to specific features of one particular structure to aid recognition.

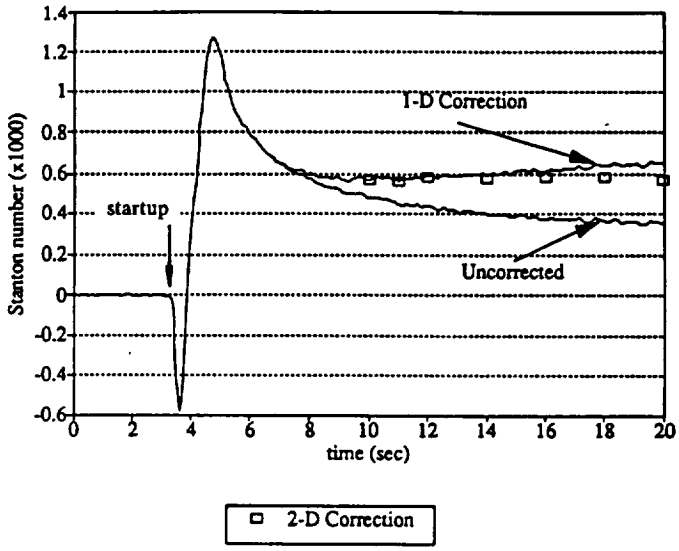

Figure 8. Stanton number variation during startup, with corrections calculated using the one-dimensional assumptions, and with corrections estimated from the NEKTON calculations.

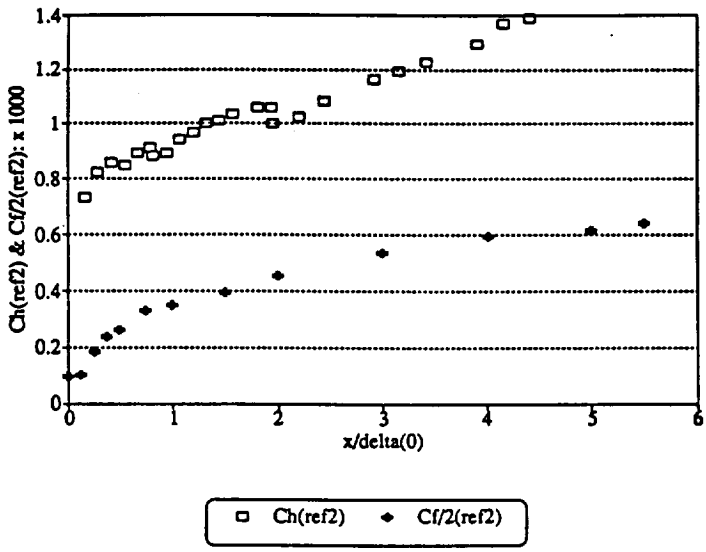

Figure 9. Corrected Stanton number and skin friction coefficient distributions along the face of the ramp, using the freestream conditions downstream of the shock.

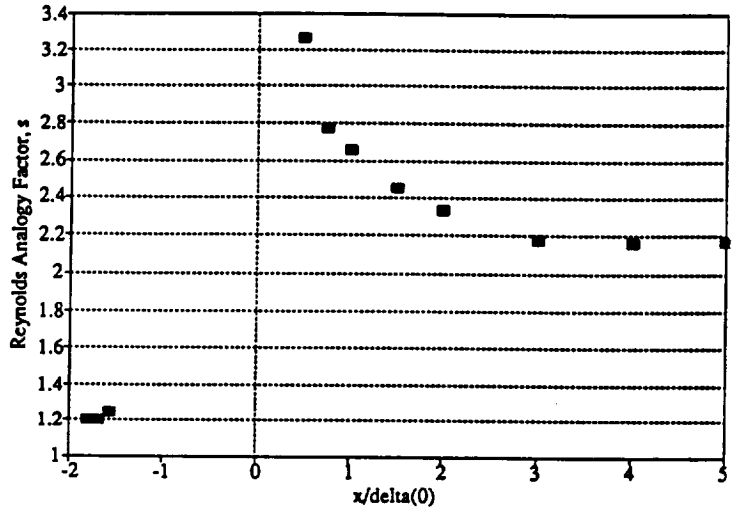

Figure 10. Distribution of the Reynolds Analogy factor in the compression ramp flow.